Figure 1. Optimization of QGP in influenza vaccine safety evaluation. A) Gene expression of *Actb, Gapdh, B2m* and *C2* and B) biomarkers, in 0.2, 2 and 20 ng RNA-containing samples from SA- and WPv-treated rat lungs. Relative expression levels of the *Gapdh* gene are indicated. SA: saline, WPv: Whole particle virion influenza vaccine.
doi:10.1371/journal.pone.0101835.g001

ers [HAv (Lot L03A) from Kaketsuken (Kumamoto), HAv (Lot 309) from Kitasato Institute (Saitama), HAv (Lot 343-A) from Denka Seiken Co., Ltd. (Tokyo), HAv (Lot HA082D) from Biken (Kagawa)] in Japan. All vaccines complied with the MRBP in Japan. HAv used in this study was tested and authorized by NCL (National Control Laboratory) for distribution in Japan.

3. Abnormal toxicity test

ATT was performed according to the MRBP [http://www.nih.go.jp/niid/en/mrbp-e.html] using rats with a slight modification.

Each 5 ml of vaccine was intra-peritoneally (*i.p.*) injected into rats. Five milliliters of saline (SA) (Otsuka normal saline; Otsuka Pharmaceutical Factory Inc., Naruto, Tokushima, Japan) was *i.p.* injected as a control. One day after the injection, rat body weight was measured and peripheral blood was collected. The number of white blood cells was counted with a hemocytometer (Nihon Kohden, Japan).
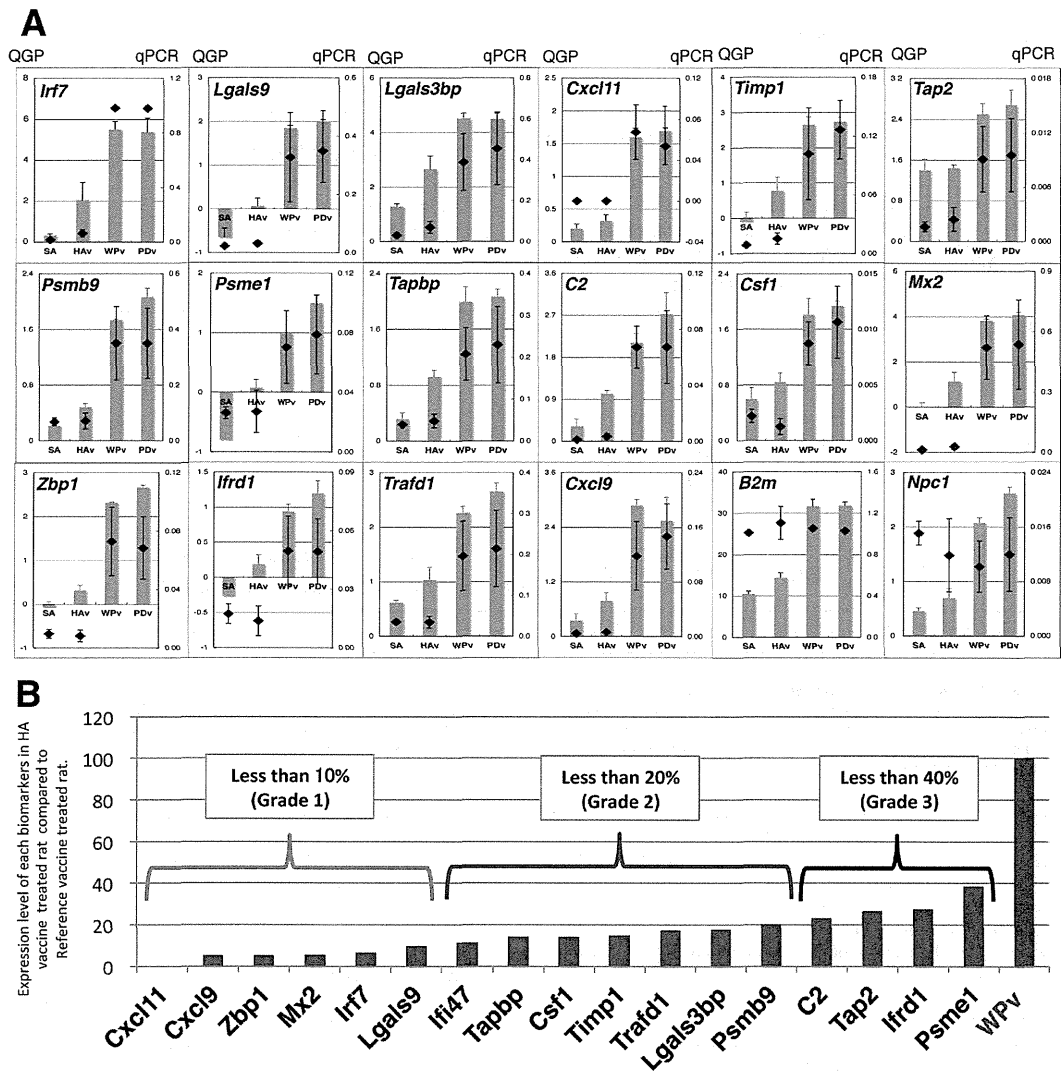
82

A

B

Figure 2. Validation of QGP with real-time PCR methods. A) GQP result was validated with real-time PCR methods. Bar graph indicates the real-time PCR results and dot blot indicates QGP results. B) Biomarkers were classified into three grades according to the relative expression level compared with WPv-treated rats.
doi:10.1371/journal.pone.0101835.g002

4. RNA preparation

One day after injection, rats were sacrificed to obtain whole lung tissues. Organs were immediately frozen in liquid nitrogen for storage. Thawed tissue was homogenized and mixed with an Isogen reagent (Nippon Gene, Tokyo, Japan). Total RNA was prepared from the lysate in accordance with the manufacturer's instructions. Poly (A)+ RNA was prepared from total RNA with a Poly (A) Purist Kit (Ambion, Austin, TX), according to the manufacturer's instructions.

5. Quantitative RT-PCR analysis

Poly (A)+ RNA was used to synthesize first-strand cDNA using a First-strand cDNA Synthesis Kit (Life Science Inc., St. Petersburg, FL), according to the manufacturer's instructions. Expression levels of biomarkers (**Table 1**) were analyzed by real-time polymerase chain reaction (PCR) using a 7500 Fast Real-Time PCR System (Applied Biosystems, Foster City, CA) with 7500 Fast System SDS Software Version 1.3. cDNA was amplified for real-time PCR using SYBR Green I (Molecular Probes Inc.) to detect the PCR products. One microliter of 6-fold diluted cDNA was
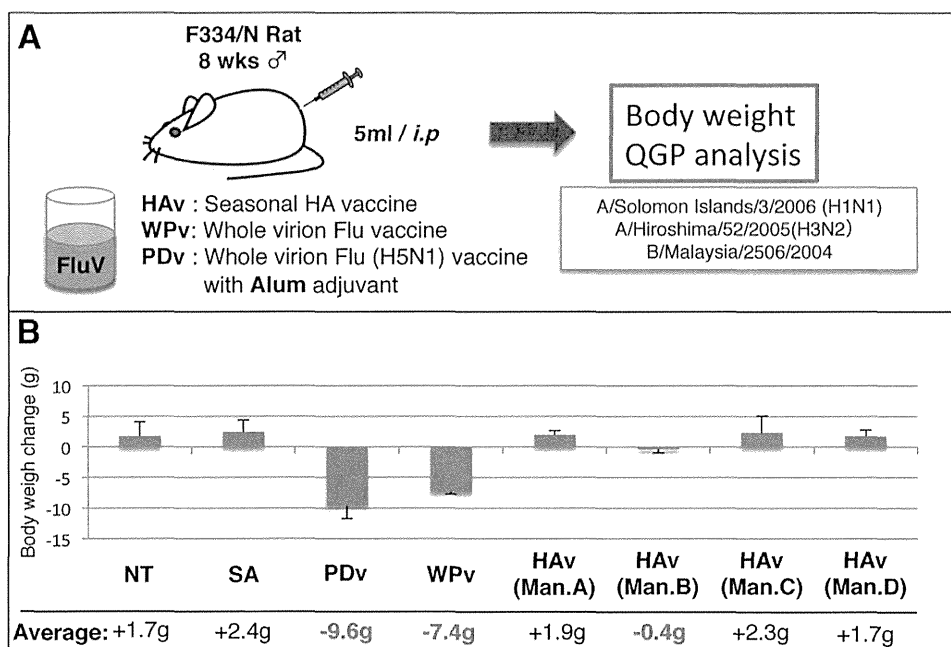
83

Figure 3. Evaluation of seasonal influenza vaccine with conventional animal safety test. A) The abnormal toxicity test was performed according to the Minimum Requirements of Biological Products. Each 5 ml vaccine was *i.p.* injected into rats, the body weight measured and lung tissues collected at day 1 after injection. B) Body weight change at day 1 after injection. NT: nontreated rat, SA: saline, PDv: pandemic H5N1 whole virion-derived vaccine with alum adjuvant, WPv: whole particle virion influenza vaccine, HAv: influenza HA vaccine, Man: manufacturer.
doi:10.1371/journal.pone.0101835.g003

used in a 20-µl final volume reaction containing 10 µl SYBR Green PCR Master Mix (Applied Biosystems), and forward and reverse primers were as described previously [13]. The 7500 Fast System was programmed to run an initial polymerase activation step at 95°C for 10 min followed by 40 cycles of denaturation (95°C for 15 s) and extension (60°C for 1 min). Product synthesis was monitored at the end of the extension step of each cycle. Gene expression values were normalized against rat GAPDH.

6. QuantiGene Plex assays

QuantiGene Plex (QGP) assays were performed according to the QuantiGene Plex Reagent System instructions (Panomics Inc., Fremont, CA), as described previously [11]. Briefly, 10 µl of starting poly (A)+RNA (50 ng) was incubated for 10 min at 65°C, then mixed with 33.3 µl of lysis mixture, 40 µl of capture buffer, 2 µl of capture beads, and 2 µl of the target gene-specific probe set. Probe sets were heated for 5 min prior to use. Each sample mixture was then dispensed into an individual well of a capture plate, sealed with foil tape and incubated at 54°C for 16–20 h. The hybridization mixture was transferred to a filter plate, and the wells were washed three times with 200 µl of wash buffer. Signals for the bound target mRNA were developed by sequential hybridization with branched DNA (bDNA) amplifier, and biotin-conjugated label probe, at 48°C for 1 h each. Two washes with wash buffer were used to remove unbound material after each hybridization step. Streptavidin-conjugated phycoerythrin was added to the wells and incubated at room temperature for 30 min. The luminescence of each well was measured using a

Luminex 100 microtiter plate luminometer (Luminex). Two replicate assays measuring RNA directly (independent sampling n = 6 for mRNA, n = 3–5 for lysate) were performed for all described experiments. The 20 target genes and GAPDH mRNA were quantified, and the ratio of the target genes to GAPDH mRNA was calculated.

7. Statistical analysis

Multiple comparisons were performed for SA, PDv, WPv and HA. To determine differences between manufacturers, multiple comparisons were performed for SA and HA from manufacturers A, B, C and D. Statistical analysis was performed in GraphPad Prism 6 (GraphPad Software, La Jolla, CA) using an ordinary one-way analysis of variance test followed by a Tukey multiple comparison test.

Results

Optimization of multiple gene detection system, QuantiGene Plex, for safety evaluation of the influenza vaccine

We previously reported that 20 selected genes (**Table 1**), from 76 differentially expressed genes in adsorbed PDv-treated rats, could be used as biomarkers to evaluate H5N1 influenza vaccine safety compared with other types of influenza vaccine using conventional real-time PCR [13]. To establish faster and more convenient methods to detect these biomarkers in one-step as a new vaccine safety test, we used QuantiGene Plex (QGP)
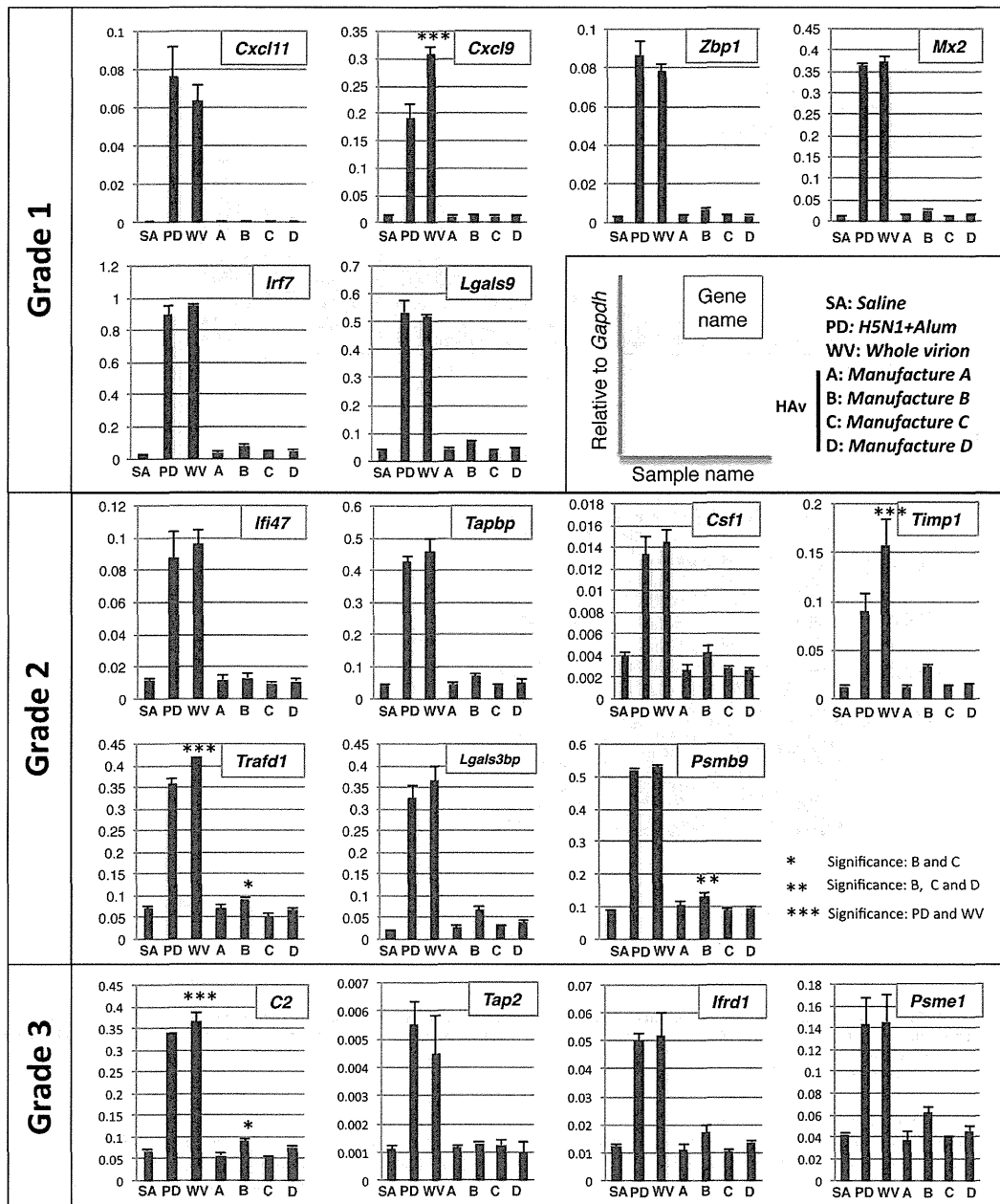
84

Figure 4. Evaluation of seasonal influenza vaccine with QGP. The relative gene expression levels of the *Gapdh* gene are indicated in each column (grades 1, 2 and 3, respectively). *Significant difference between B and C. **Significant difference between B, C and D, ***Significant difference between PD and WPv.
doi:10.1371/journal.pone.0101835.g004

technology (Panomics Inc., Fremont, CA). We designed a custom QGP 2.0 assay to enable the measurement of expression levels of

identified biomarkers. The Panomics QGP 2.0 assays provided quantitative measurements of 3 to 80 target RNAs per well by
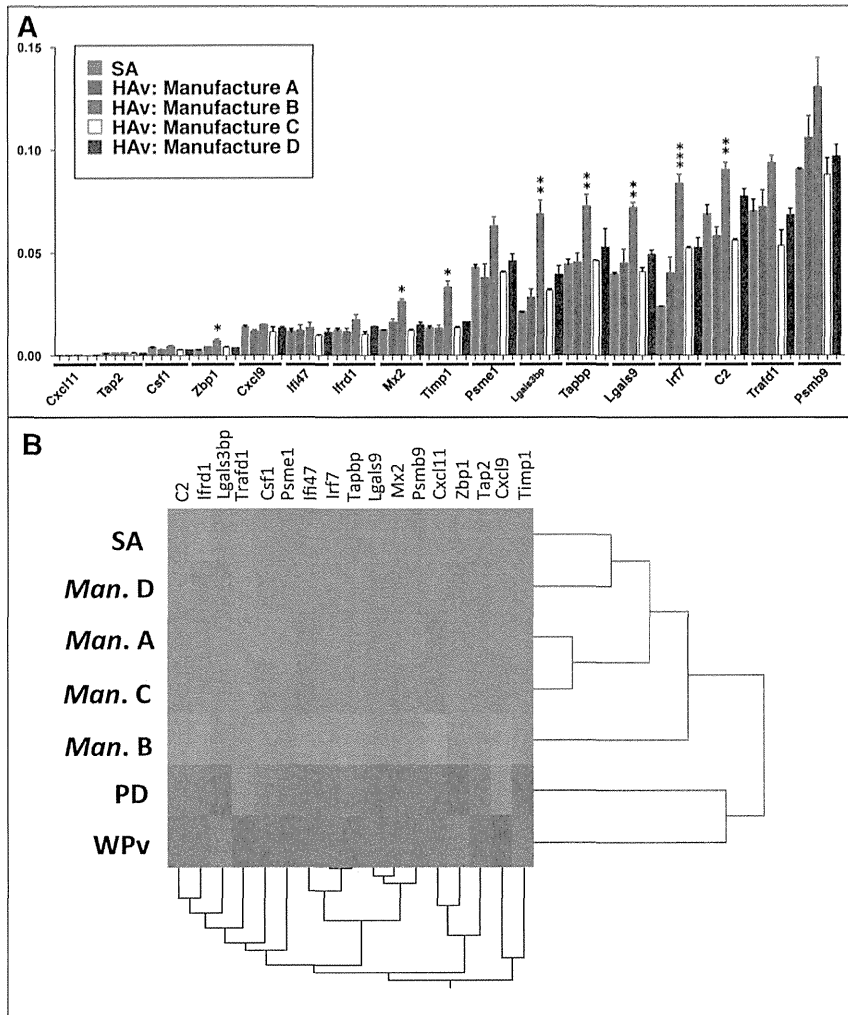
85

Figure 5. Evaluation of seasonal influenza vaccine with QGP and cluster analysis. A) Relative gene expression in HAv-treated rat lungs to *Gapdh* is indicated in the bar graph. B) Hierarchical clustering analysis with biomarkers could predict differences in HAv manufacturers as B is located in a separate cluster from other HAvs.
doi:10.1371/journal.pone.0101835.g005

using bDNA technology in conjunction with multi-analyte magnetic beads to provide the detection and quantitation of multiple mRNA targets simultaneously. bDNA technology is a hybridization-based methodology that uses labeled DNA probes to amplify the signal rather than the target mRNA. Here, we produced probes for 20 genes and two control genes (*Actb* and *Gapdh*) for the one-step detection and quantification of these biomarkers. To check the sensitivity of probes and dynamic range of our biomarkers, we prepared 0.02, 0.2, 2 and 20 ng total RNA samples from WPv and SA-treated rat lungs and performed QGP analysis. Two control genes and two biomarkers ($\beta 2m$ and *C2*) reacted in a dose-dependent manner (**Figure 1A**). We re-

evaluated all probes with the same sample. Each biomarker reacted in a dose-dependent manner (**Figure 1B**) except *Ngfr* and *Npc1*. Therefore, 20 ng of RNA sample was used for multiplex gene detection. All biomarkers except $\beta 2m$ reacted in a dose-dependent manner. $\beta 2m$ was saturated when using 20 ng RNA sample; thus $\beta 2m$ could not be used for QGP analysis.

Validation of QGP with real-time PCR

To validate QGP, we performed real-time PCR analysis using the same samples. As a result, most biomarker gene expression data from the QGP correlated with the real-time PCR result except for $\beta 2m$, *Npc1* (Figure 2) and *Ngfr* (data not shown). Finally,
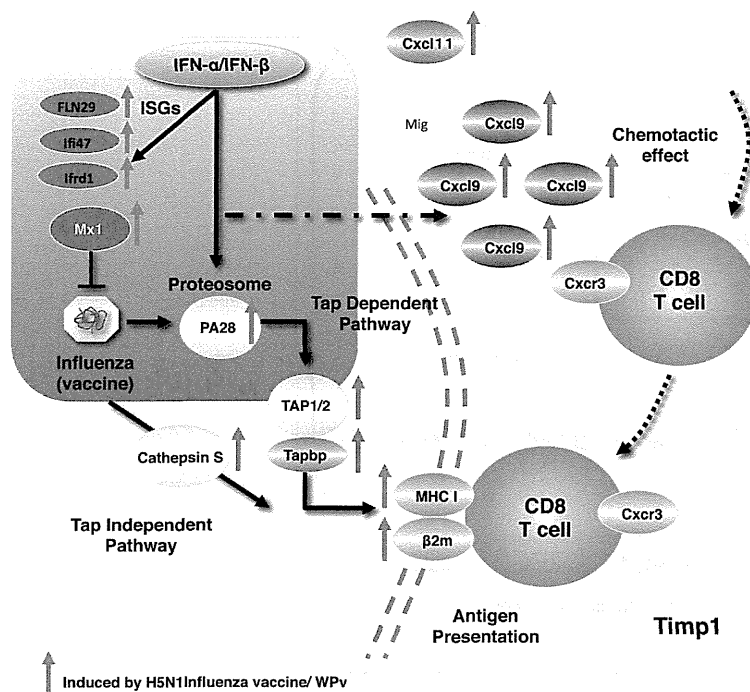
Figure 6. Summary of biomarker studies. Biomarkers used in this study were strongly correlated with immune responses after influenza infection.
doi:10.1371/journal.pone.0101835.g006

17 genes were selected as the multiplex detection biomarker set. We next determined the relative biomarker expression levels in HAv-treated rat lungs compared with WPv used as a reference toxicity vaccine in the leukopenic toxicity test (LTT) in Japan. We classified *Cxcl11*, *Cxcl9*, *Zbp1*, *Mx2*, *Irf7* and *Lgals9* as a "Grade 1" gene set where relative expression levels in HAv compared with WPv were less than 10%. Likewise, we classified *Ifi47*, *Tapbp*, *Csf1*, *Timp1*, *Trafd1*, *Lgals3bp* and *Psmb9* as a "Grade 2" gene set where relative expression levels were less than 20% and *C2*, *Tap2*, *Ifrd1* and *Psme1* as a "Grade 3" gene set where relative expression levels were less than 40% in HAv compared with WPv. In Japan, it is acceptable for leukopenic toxicity levels of HAv to be not more than 20% of WPv by LTT. We applied LTT criteria for selecting and subdividing these biomarkers into three grades with expression levels below 20% of WPv and others.

Evaluation of HAv safety in Japan using ATT and QGP

To evaluate the toxicity of seasonal HAv using biomarkers, we purchased market authorized seasonal influenza vaccines distributed in Japan from four different manufacturers (Kaketsuken, Denka Seiken, Kitasato, and Biken). Although the vaccines have been evaluated and passed ATT by the NCL according to the Japanese guidelines for MRBP, the reactogenicity of the vaccine to animals (rats, mice and guinea pigs) was varied. To evaluate these differences, we performed ATT and checked the body weight changes of rats after i.p. injection of each HAv (Figure 3A). Although treatment with PDv or WPv (toxic reference whole virion-derived vaccines) significantly decreased the body weight of

rats, HAvs from three different manufacturers had no effect on body weight. HAv from manufacture B reduced the body weight of rats at day 1 (Figure 3B). However, there was no significant difference in rat body weight change for the other HAvs; thus HAv from manufacturer B might be slightly different, when comparing the mean body weight at day 1. In addition, there was no significant difference in leukocyte numbers following administration of HAv from the four manufacturers (data not shown). To evaluate the differences of each HAv, we next performed multiplex biomarker detection by QGP. No biomarkers were significantly up-regulated in HAv-treated rats compared with controls (Figure 4) except for *Psmb9*. Furthermore, *Psmb9* expression was significantly up-regulated following administration of HAv from manufacturer B compared with the control SA-treated and HAvs from the other manufacturers. The expression levels of *C2* and *Trafd1* were also significantly up-regulated in the HAv from manufacturer B compared with the HAv from manufacturer C.

Biomarkers to evaluate safety of adjuvanted influenza vaccine

Both PDv and WPv contain the whole virion influenza vaccine and alum adjuvant is only added to PDv to enhance its immunogenicity. There was no difference in body weight change between WPv- and PDv-treated rats (Figure 3B). However, among the 17 biomarkers, the expression level of three genes, *Cxcl9*, *Timp1* and *Trafd1* in PDv-treated rats were significantly decreased compared with WPv-treated rats (Figure 4). Thus, these biomarkers could potentially evaluate the aluminum adjuvant effect.
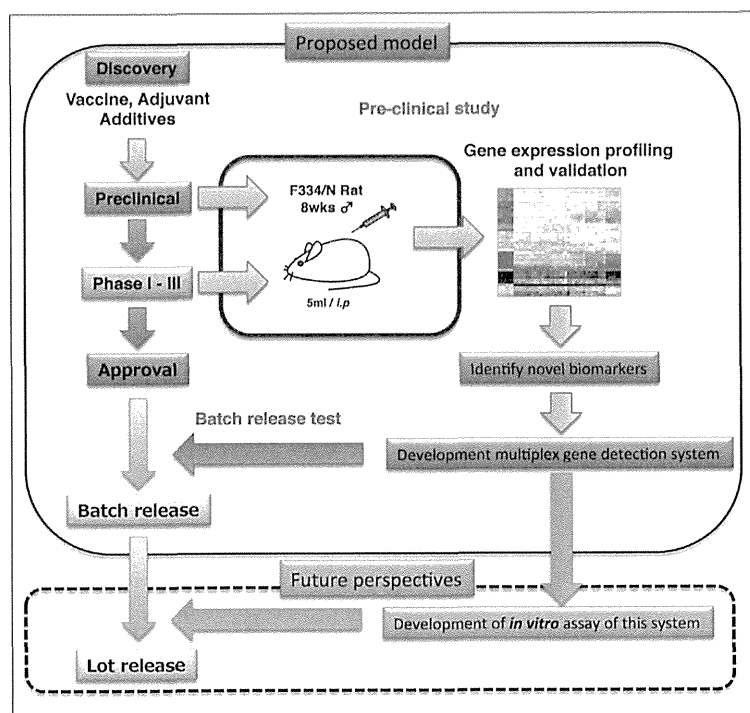
8

87

Figure 7. Application of the system biological approach for influenza vaccine development. Proposed model of future influenza vaccine development and establishment of preclinical studies and batch release testing. Acquisition of transcriptome data at the preclinical and clinical phase is useful for future batch release testing and the prediction of vaccine efficacy and toxicity.
doi:10.1371/journal.pone.0101835.g007

Cluster analysis of QGP data predicts influenza vaccine safety

Conventional animal tests such as ATT and LTT have been performed in Japan for the evaluation of influenza vaccine safety and toxicity. Despite applying these tests that evaluate whole virion-derived influenza vaccine from HAv, it is difficult to distinguish statistically between different HAvs if they do not have comparable toxicity greater than 20–50% to WPv. According to the body weight change observed with ATT, we speculated that HAv from manufacturer B was slightly different than the others tested (Figure 3B), although this was not statistically significant. However, when biomarkers were used with QGP to evaluate HAvs, we could distinguish the HAv from manufacturer B compared with those from other manufacturers. When we focused on biomarker expression among the HAv-treated rat lungs, the expression levels of *Zbp1*, *MX2*, *Timp1*, *Lgals3bp*, *Tapbp*, *Lgals9*, *Irf7* and *C2* were significantly up-regulated in rat lungs treated with HAvs from manufacturer B (Figure 5A). In addition, cluster analysis with the biomarkers predicted differences in HAvs as the vaccine from manufacturer B was located in a separate cluster from the other HAvs. Thus, these biomarkers can evaluate batch-to-batch and manufacturer-to-manufacturer differences in HAvs (Figure 5B).

Discussion

Vaccine safety is critical in the process of vaccine development and universal vaccination. Several vaccines were stopped owing to safety concerns, including severe side effects, after they had received marketing authorization and licensing, even when they were effective [14]. To ensure the safety of vaccines, the preclinical phase in the development of vaccines and the batch release system after marketing authorization is critical. However, the guidelines for nonclinical assessment of vaccines and batch release tests only focus on the evaluation of vaccine efficacy and immunogenicity in animal models, quality control testing programs and toxicology testing in relevant animal models [15]. These guidelines do not include scientific research for identifying the potential toxicities of the vaccines, adjuvants and additives.

We have demonstrated the advantage of a system biological approach using several vaccines authorized in Japan, e.g. DPT, JEV and Influenza vaccine including H5N1 pandemic influenza vaccine [10–13]. We successfully identified several biomarkers to evaluate DPT, JEV and influenza vaccine toxicity. In this study, we demonstrate that the biomarkers used to evaluate H5N1 pandemic influenza vaccine could also be used to evaluate the batch-to-batch consistency and the safety of HAvs. In addition, they can be used to evaluate manufacturer-to-manufacturer differences using the multiplex gene detection system. The biomarker analysis correlated to findings from conventional

88

animal use tests, such as ATT. In addition, sensitivity of toxicity detection and differences in HAvs was higher and more accurate than with conventional methods. Despite all the HAvs evaluated in this study meeting MRBP criteria and passing NCL, our results suggest that HAv from manufacturer B is slightly different than the HAvs according to *Lgals3bp*, *Tapbp*, *Lgals9*, *Irf7* and *C2* gene expression. Among the official vaccine adverse event information provided by the Japanese authorities, there is no reported evidence that the adverse event rate was increased or that severe adverse events were observed caused by HAv from manufacturer B. It is still unknown what factors (additives, formalin content, protein content) induce these biomarkers in the HAv from manufacturer B. Further studies are needed to determine whether our biomarkers could predict the toxicity of influenza vaccine by using different formulations of HAv. Using biomarkers from any grade characterized in this study, we could also predict the safety of influenza vaccines within 2 days whereas the conventional animal use safety test, ATT requires 7 days for evaluating batch-to-batch consistency and vaccine safety. Further studies are needed to determine how these biomarkers can be used to evaluate the safety of HAv. To set the percent limit of up-regulation of each biomarker, it might be helpful to compare another conventional test such as LTT [[http://www.nih.go.jp/niid/en/mrbp-e.html]] as well as a comparison of failed batches of HAv. LTT evaluates the peripheral leukocyte number reduction rate compared with WPv. In general, WPv induces a strong loss of peripheral leukocyte numbers 16 hours after WPv administration in mice [9 and 28]. The test criteria of LTT is that the loss of leukocyte numbers in test samples must be no greater than 20% compared with a reference toxic vaccine such as WPv or less than 50% of SA-treated mice. These criteria may be applicable to set our biomarker expression limit. Further validation is required to set the limit the gene expression level.

Influenza is a socially important infectious disease that causes seasonal flu outbreaks worldwide and has a pandemic status [16]. Correspondingly, many types of influenza vaccine (cell derived, recombinant derived, live attenuated and inactivated influenza vaccine), have been developed to ensure efficacy and reduce toxicity [17]. While some adjuvants have been developed and used to amplify vaccine efficacy [8], the safety of adjuvants is still of concern. Recently, several adjuvants (squalene-based MF59 and AS03) developed and licensed for use only in pandemic influenza vaccines were under investigation for the occurrence of narcolepsy in vaccinated children in European countries [18]. Conventional safety tests could be used to evaluate the safety of these vaccines [19], but it is still difficult to predict the safety and toxicity of influenza vaccines, adjuvants and additives [20]. We demonstrated that usage of system biological approaches to evaluate safety might revolutionize vaccine testing methods [21]. Most of the previously identified biomarkers were up-regulated and correlated with influenza infection, interferon responses, antigen presentation and antibody production (Figure 6). In addition, we found that several biomarkers, *Cxcl9*, *Trafd1*, and *C2* were candidates for evaluating differences between alum-adjuvanted influenza vac-

cines and nonadjuvanted vaccines. Further studies, using several adjuvants, are needed to confirm the feasibility of these biomarkers in evaluating adjuvant safety.

In addition to whole transcriptome analysis of vaccinated animals, recent advances in genome research enabled the acquisition of whole transcriptional data from vaccinated individuals and identification of gene expression after immunization with vaccines to yellow fever, measles, tularemia and tuberculosis [22]. With a focus on the influenza vaccine, Bucasas et al. reported a 494 gene set, including biomarkers identified in our previous study (*MX1*, *IRF7*) that strongly correlated with antibody responses in humans [23]. Wei et al. reported gene expression differences between HAv and live attenuated influenza vaccine. They identified 265 differentially expressed genes, including our previously identified biomarkers, *IRF7*, *MX1*, *MX2*, *OAS1* and *ZBP1* [24].

Recently, Nakaya and Pulendran reported a system biological approach, termed systems vaccinology [25], which was used to predict immunogenicity and provide new mechanistic insights regarding influenza vaccination. They also reported several gene sets that predicted influenza vaccine immunogenicity, including our previously identified biomarkers, *MX1*, *MX2*, *OAS1* and *IRF7* [26]. More recently, Franco et al. reported 20 genes, including our biomarkers, *TAP2* and *OAS1*, which correlated with antibody responses, using integrative genomic analysis [27]. All these reports suggest that using animal models is still useful if biomarkers are up-regulated in vaccinated individuals and can reveal the role of biomarkers in immune responses and vaccination toxicity. Thus, in the preclinical and clinical phase, the acquisition of transcriptome data from both vaccinated individuals and animals, and a comparison of these data will be helpful for future vaccine development and batch release testing (Figure 7).

Taken together, system biological approaches to identify vaccine toxicity using whole genome transcriptome methods will improve vaccine development in preclinical and clinical phases if more data are generated from successfully vaccinated individuals and those with side effects. It is still unclear whether and how these factors determine immunogenicity and toxicity. Further studies are required to identify and reveal the mechanisms underlying vaccination in humans and in animal models, including nonhuman primates.

Acknowledgments

Author Contributions

Conceived and designed the experiments: TM. Performed the experiments: TM HM MK KT. Analyzed the data: TM HM KJI IH KY. Contributed reagents/materials/analysis tools: TM HM MK KT KA KF KJI. Wrote the paper: TM.

References

1. Plotkin SL, Plotkin SA (2012) A short history of vaccination. General aspects of vaccination. In: Plotkin SA, Orenstein WA, Offit PA, editors. 6th edition Vaccines. Philadelphia: Saunders Elsevier. 1–13.
2. Baylor NW, Marshall VB (2012) Regulation and testing of vaccines. In: Plotkin SA, Orenstein WA, Offit PA, editors. 6th edition Vaccines. Philadelphia: Saunders Elsevier. 1427–1446.
3. Kurokawa M, Murata R (1961) On the Toxicity of the Toxoid Preparation Responsible for the Kyoto Catastrophe in 1948. Jpn J Med Sci Biol 14: 249–256.
4. Wood JM, Williams MS (1998) History of inactivated influenza vaccines. In: Nicholson KG, Webster RG, Hay AJ, editors. Textbook of influenza. Oxford: Blackwell Science. 317–323.
5. Nicholson KG, Tyrrell DA, Harrison P, Potter CW, Jennings R, et al. (1979) Clinical studies of monovalent inactivated whole virus and subunit A/USSR/77 (H1N1) vaccine: Serological responses and clinical reactions. J Biol Stand 7: 123–136.
6. Wright PF, Thompson J, Vaughn WK, Folland DS, Sell SH, et al. (1977) Trials of influenza A/New Jersey/76 virus vaccine in normal children: an overview of age-related antigenicity and reactogenicity. J Infect Dis 136: S731–S741.

89

7. Couch RB, Keitel WA, Cate TR (1997) Improvement of inactivated influenza virus vaccines. J Infect Dis. 176 Suppl 1: S38–44.

8. Even-Or O, Samira S, Ellis R, Kedar E, Barenholz Y (2013) Adjuvanted influenza vaccines. Expert Rev Vaccines. 12: 1095–1108.

9. Mizukami T, Masumi A, Momose H, Kuramitsu M, Takizawa K, et al. (2009) An improved abnormal toxicity test by using reference vaccine-specific body weight curves and histopathological data for monitoring vaccine quality and safety in Japan. Biologicals. 37: 8–17.

10. Hamaguchi I, Imai J, Momose H, Kawamura M, Mizukami T, et al. (2007) Two vaccine toxicity-related genes Agp and Hpx could prove useful for pertussis vaccine safety control. Vaccine. 25: 3355–3364.

11. Hamaguchi I, Imai J, Momose H, Kawamura M, Mizukami T, et al. (2008) Application of quantitative gene expression analysis for pertussis vaccine safety control. Vaccine. 26: 4686–4696.

12. Momose H, Imai J, Hamaguchi I, Kawamura M, Mizukami T, et al. (2010) Induction of indistinguishable gene expression patterns in rats by Vero cell-derived and mouse brain-derived Japanese encephalitis vaccines. Jpn J Infect Dis. 63: 25–30.

13. Mizukami T, Imai J, Hamaguchi I, Kawamura M, Momose H, et al. (2008) Application of DNA microarray technology to influenza A/Vietnam/1194/ 2004 (H5N1) vaccine safety evaluation. Vaccine. 26: 2270–2283.

14. Offit PA, Stefano FD (2012) Vaccine safety. In: Plotkin SA, Orenstein WA, Offit PA, editors. 6th edition Vaccines. Philadelphia: Saunders Elsevier. 1464–1480.

15. Wolf JJ, Kaplanski CV, Lebron JA (2010) Nonclinical safety assessment of vaccines and adjuvants. Methods Mol Biol. 626: 29–40.

16. WHO (2013) Pandemic Influenza Risk Management, WHO Interim Guidance. Available: http://www.who.int/influenza/preparedness/pandemic/GIP_ PandemicInfluenzaRiskManagementInterimGuidance_Jun2013.pdf. Accessed 2014 June 18.

17. Wong SS, Webby RJ (2013) Traditional and new influenza vaccines. Clin Microbiol Rev. 26: 476–492.

18. Ahmed SS, Schur PH, Macdonald NE, Steinman L (2014). Narcolepsy, 2009 A (H1N1) pandemic influenza, and pandemic influenza vaccinations: What is known and unknown about the neurological disorder, the role for autoimmunity, and vaccine adjuvants. J Autoimmun. 50: 1–11.

19. Brennan FR1, Dougan G (2005) Non-clinical safety evaluation of novel vaccines and adjuvants: new products, new strategies. Vaccine. 23: 3210–3222.

20. Verdier F, Morgan L (2001) Predictive value of pre-clinical work for vaccine safety assessment. Vaccine. 20 Suppl 1: S21–23.

21. Momose H, Mizukami T, Ochiai M, Hamaguchi I, Yamaguchi K (2010) A new method for the evaluation of vaccine safety based on comprehensive gene expression analysis. J Biomed Biotechnol. 2010: 361841.

22. Wang IM, Bett AJ, Cristescu R, Loboda A, ter Meulen J (2012) Transcriptional profiling of vaccine-induced immune responses in humans and non-human primates. Microb Biotechnol. 5: 177–187.

23. Bucasas KL, Franco LM, Shaw CA, Bray MS, Wells JM, et al. (2011) Early patterns of gene expression correlate with the humoral immune response to influenza vaccination in humans. J Infect Dis. 203: 921–929.

24. Zhu W, Higgs BW, Morehouse C, Streicher K, Ambrose CS, et al. (2010) A whole genome transcriptional analysis of the early immune response induced by live attenuated and inactivated influenza vaccines in young children. Vaccine. 28: 2865–2876.

25. Pulendran B, Li S, Nakaya HI (2010) Systems vaccinology. Immunity. 33: 516–529.

26. Nakaya HI, Wrammert J, Lee EK, Racioppi L, Marie-Kunze S, et al. (2011) Systems biology of vaccination for seasonal influenza in humans. Nat Immunol. 12: 786–795.

27. Franco LM, Bucasas KL, Wells JM, Niño D, Wang X, et al. (2013) Integrative genomic analysis of the human immune response to influenza vaccination. Elife. 2: e00299.

28. Ato M, Takahashi Y, Fujii H, Hashimoto S, Kaji T, et al. (2013) Influenza A whole virion vaccine induces a rapid reduction of peripheral blood leukocytes via interferon-α-dependent apoptosis. Vaccine. 31: 2184–2190.

90

B-Cell-Intrinsic Hepatitis C Virus Expression Leads to B-Cell-Lymphomagenesis and Induction of NF-κB Signalling

Yuri Kasama[1], Takuo Mizukami[2], Hideki Kusunoki[2], Jan Peveling-Oberhag[3], Yasumasa Nishito[4], Makoto Ozawa[6,7], Michinori Kohara[5], Toshiaki Mizuochi[2], Kyoko Tsukiyama-Kohara[6,7]*

1 Department of Experimental Phylaxiology, Faculty of Life Sciences, Kumamoto University, Kumamoto-shi, Kumamoto, Japan, 2 Department of Research on Blood and Biological Products, National Institute of Infectious Diseases, Musashi-Murayama-shi, Tokyo, Japan, 3 Department of Internal Medicine, Goethe-University Hospital, Frankfurt, Germany, 4 Center for Microarray Analysis, Tokyo Metropolitan Institute of Medical Science, Kamikitazawa, Tokyo, Japan, 5 Department of Microbiology and Cell Biology, Tokyo Metropolitan Institute of Medical Science, Kamikitazawa, Tokyo, Japan, 6 Transboundary Animal Diseases Center, Joint Faculty of Veterinary Medicine, Kagoshima University, Kagoshima, Japan, 7 Laboratory of Animal Hygiene, Joint Faculty of Veterinary Medicine, Kagoshima University, Kagoshima, Japan

Abstract

Hepatitis C virus (HCV) infection leads to the development of hepatic diseases, as well as extrahepatic disorders such as B-cell non-Hodgkin's lymphoma (B-NHL). To reveal the molecular signalling pathways responsible for HCV-associated B-NHL development, we utilised transgenic (Tg) mice that express the full-length HCV genome specifically in B cells and develop non-Hodgkin type B-cell lymphomas (BCLs). The gene expression profiles in B cells from BCL-developing HCV-Tg mice, from BCL-non-developing HCV-Tg mice, and from BCL-non-developing HCV-negative mice were analysed by genome-wide microarray. In BCLs from HCV-Tg mice, the expression of various genes was modified, and for some genes, expression was influenced by the gender of the animals. Markedly modified genes such as Fos, C3, LTβR, A20, NF-κB and miR-26b in BCLs were further characterised using specific assays. We propose that activation of both canonical and alternative NF-κB signalling pathways and down-regulation of miR-26b contribute to the development of HCV-associated B-NHL.

Introduction

Approximately 200 million people are currently infected with the hepatitis C virus (HCV) worldwide [1]. HCV has been the major etiological agent of post-transfusion hepatitis and has frequently caused liver cirrhosis and hepatocellular carcinoma in chronic hepatitis C (CHC) patients [2,3]. Hepatocytes are considered to be the primary and major site of HCV replication; however, extrahepatic manifestations are commonly seen in CHC patients. For example, mixed cryoglobulinemia (MC), a systemic immune complex-mediated disorder characterised by B cell proliferation with the risk of evolving into overt B-cell non-Hodgkin's lymphoma (B-NHL), is frequently recognised in CHC patients [4–6]. We have previously demonstrated the presence of both HCV RNA and viral proteins in peripheral B cells of CHC patients [7], although the mode of HCV infection and possible HCV replication in peripheral B cells remains a matter of debate. Furthermore, in the last two decades, an array of epidemiological evidence has accumulated involving the association between HCV infection and the occurrence of several hematologic malignancies, most notably B-NHL [8], [9]. The most compelling argument for a causal relationship between HCV and the occurrence of B-NHL is made by interventional studies demonstrating that a sustained

virologic response to antiviral treatments, including the interferon α-induced regression of HCV-associated lymphomas and viral relapse after the initial virologic response, led to lymphoma recurrence [10]. However, the mechanisms underlying the cause-and-effect relationship are mostly unknown.

One of the potential host factors involved in HCV-associated B-NHL development is activator protein 1 (AP-1), which is primarily composed of c-Jun, c-Fos, and JunB, while JunD or Fra-1, Fra-2 and FosB are involved less frequently [11]. AP-1 is involved in B cell lymphomagenesis, is repressed by B cell lymphoma-6 [12] and is inhibited by the overexpression of T cell leukaemia/lymphoma 1, which resulted in the enhancement of nuclear factor kappa B (NF-κB) [13].

NF-κB is a ubiquitously expressed transcription factor that regulates a wide array of cellular processes, including the immune response, cell growth and differentiation [14,15]. The activation of NF-κB is regulated by two distinct pathways termed the 'canonical' and the 'alternative' NF-κB signalling pathways. Representative stimulators of the canonical and alternative pathways are tumour necrosis factor αTNFα) and lymphotoxin α and β (LTα and LTβ), respectively [16]. Previous studies have demonstrated that NF-κB is activated via both the canonical [17,18] and alternative [19] pathways in chronic HCV infection

91

[17,18] and HCV-related B-NHL [20]. However, the key NF-κB-activating pathway involved in HCV-associated B-NHL remains unknown.

TNFα-induced protein 3 (TNFAIP3), also known as A20, was first identified as a TNF-induced cytoplasmic protein with zinc finger motifs [21]. A20 has since been described as playing a pivotal role in the negative regulation of inflammation by terminating the canonical NF-κB signalling pathway [22–24]. Recently, A20 has gained attention as a novel tumour suppressor. For example, A20 was reported to be frequently inactivated or even deleted from mantle-cell lymphoma [25,26] and diffuse large B-cell lymphoma (DLBCL) [27]. These findings raise the possibility that inactivation of A20 is, at least partially, responsible for lymphomagenesis [28–30]. Other investigators have subsequently confirmed these findings [27,31]. Moreover, A20 also regulates antiviral signalling [32] as well as programmed cell death [33–35].

microRNAs (miRNAs) play a role in controlling various biological functions, including cell differentiation, growth regulation and transcriptional regulation [36]. In general, the dysfunctional expression of miRNAs is considered to be a common hallmark of cancers, including lymphomas [37]. HCV has been shown to influence miRNA expression in vivo and in vitro and utilises the liver-specific microRNA miR-122 for its replication [38]. The expression of miRNAs is also known to involve NF-κB activation. For example, miR-125a and miR-125b, both of which are often duplicated and/or overexpressed in DLBCL, were shown to activate NF-κB by targeting the A20 [39] and NF-κB-mediated dysregulation of miRNAs observed in lymphoma[40]. Moreover, global miRNA expression profiling analysis revealed miR-26b down-regulation in HCV-related splenic marginal zone lymphomas (SMZL) [41]. The same miRNA was found to be downregulated in peripheral blood mononuclear cells (PBMCs) from HCV-positive MC and NHL subjects [42].

We recently established transgenic mice that express the full-length HCV genome specifically in B cells (HCV-Tg mice) and observed the incidence of non-Hodgkin type B-cell lymphoma (BCL), primarily DLBCL, within 600 days after birth in approximately 25% of the HCV-Tg mice [43]. This experimental model is a useful tool for analysing the mechanisms underlying the development of HCV-associated manifestations such as B-NHL. To reveal the molecular signalling pathways responsible for HCV-associated B-NHL development, we performed a comprehensive molecular analysis of BCLs in HCV-Tg mice using a genome-wide microarray. We also characterised miR-26b expression in BCLs from HCV-Tg mice. Our results suggest that the activation of both canonical and alternative NF-κB pathways is involved in HCV-associated B-NHL development.

Materials and Methods

Ethics Statement

This study was carried out in strict accordance with both the Guidelines for Animal Experimentation of the Japanese Association for Laboratory Animal Science and the Guide for the Care and Use of Laboratory Animals of the National Institutes of Health. All experiment protocols were approved by the institutional review boards of the regional ethics committees of Kumamoto University (A22-136) and Kagoshima University (H24-008).

Animal experiments

The full-length HCV genome (Rz) under the conditional Cre/loxP expression system [44] with mice expressing the Cre enzyme

under the transcriptional control of the B lineage–restricted gene CD19 [45] was established as RzCD19Cre mice [43]. Wild-type (WT), Rz, CD19Cre, RzCD19Cre mice (129/sv, BALB/c and C57BL/6J mixed background) were maintained in conventional animal housing under specific pathogen-free conditions. CD19Cre and RzCD19Cre mice were bred to be heterozygous for the Cre allele.

Isolation of B cells and their RNAs

Mouse B cells were isolated using MACS^R beads (Milteny Biotec, Bergisch Gladbach, Germany) and anti-CD19 antibody (Beckton Dickinson, Franklin Lake, NJ). For FACS analysis, B and T cell populations were characterised using FITC-conjugated anti-B220 antibody (Milteny Biotec) and phycoerythrin (PE)-conjugated anti-CD3 antibody (Milteny Biotec) (Figure S1A). B cell purity was routinely over 95%. Total RNA was extracted from the B cells using the acid guanidine thiocyanate phenol chloroform method [44,46]. The RNA integrity number was measured with an Agilent 2100 Bioanalyzer (Agilent Technologies, Santa Clara, CA), and samples with values over 8.0 were subjected to microarray analysis (Figure S1B).

Microarray analysis

For microarray analysis, total RNAs were extracted, and RNA integrity was assessed using a Bioanalyzer (Agilent Technologies). cRNA targets were synthesised and hybridised with Whole Mouse Genome Microarray (G4846A; Agilent Technologies), in accordance with the manufacturer's instructions. More than 2-fold changes in gene expression were considered to be significant. Array data were analysed using MetaCore™ software (Thomson Reuters Co., New York, NY). The results of microarray analysis

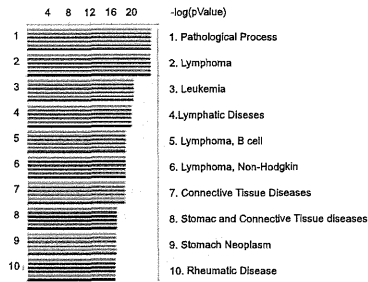**Table 1.** Mice subjected to microarray analysis.

Pairing	Mouse genotype	Mouse (No)	Age (d)	Sex	Remarks
1	RzCD19Cre	24–1	748	male	HCV(+)BCL*
		59–1	723	male	
		69–5	710	male	
	RzCD19Cre	248–1	860	male	HCV(+) B cell
		288–3	472	male	
		299–1	385	male	
2	RzCD19Cre	307–2	212	male	HCV(+) B cell
		307–3	212	male	
	Rz, 4EBP(+/−)†	307–1	220	male	HCV(−) B cell
		312–1	220	male	
3	RzCD19Cre	54–1	724	female	HCV(+)BCL
		62–2	723	female	
	RzCD19Cre	308–4	219	female	HCV(+) B cell
		308–6	219	female	
4	RzCD19Cre	308–4	219	female	HCV(+) B cell
		308–6	219	female	
	Rz	308–1	219	female	HCV(−) B cell
		308–3	219	female	

*BCL: B cell lymphoma; †4EBP(+/−): heterozygous knockout of 4E-BP1 gene [73].
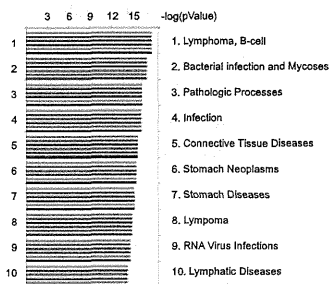doi:10.1371/journal.pone.0091373.t001

92

A Disease network
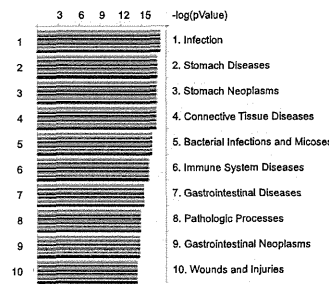
Pairing1 (HCV+B vs HCV+BCL, male)

-log(pValue)   4 8 12 16 20

1. Pathological Process
2. Lymphoma
3. Leukemia
4. Lymphatic Diseses
5. Lymphoma, B cell
6. Lymphoma, Non-Hodgkin
7. Connective Tissue Diseases
8. Stomac and Connective Tissue diseases
9. Stomach Neoplasm
10. Rheumatic Disease

Pairing 2 (HCV+ vs HCV-, B cells, male)

-log(pValue)   5 10 15 20 25 30

1. Wounds and Injuries
2. Bacterial Infections ans Mycoses
3. Infection
4. Musculoskeletal Diseases
5. Arthritis, Rheumatoid
6. Rheumatic Diseases
7. Connective Tissue Diseases
8. Inflamation
9. Autoimmune Diseases
10. Patholodic Processes

Pairing3 (HCV+B vs HCV+BCL, female)

-log(pValue)   3 6 9 12 15

1. Lymphoma, B-cell
2. Bacterial infection and Mycoses
3. Pathologic Processes
4. Infection
5. Connective Tissue Diseases
6. Stomach Neoplasms
7. Stomach Diseases
8. Lympoma
9. RNA Virus Infections
10. Lymphatic Diseases

Pairing 4 (HCV+ vs HCV-, B cells, female)

-log(pValue)   3 6 9 12 15

1. Infection
2. Stomach Diseases
3. Stomach Neoplasms
4. Connective Tissue Diseases
5. Bacterial Infections and Micoses
6. Immune System Diseases
7. Gastrointestinal Diseases
8. Pathologic Processes
9. Gastrointestinal Neoplasms
10. Wounds and Injuries

B Process network

Pairing1 (HCV+B vs HCV+BCL, male)

-log(pValue)   2 4 6 8 10

1. Cell cycle_Mitosis
2. Cell adhesion_Leucocyte chemotaxis
3. Immune response_BCR pathway
4. Immune response_TCR signalung
5. Cell cycle_Core
6. Inflammation_IL-2 signaling
7. Cytoskelton_Regulation of cytoskelton rearangement
8. Cell cycle_G2-M
9. Inflammation_IFN-gamma signaling
10. Cytoskelton_spindle microtubles

Pairing 2 (HCV+ vs HCV-, B cells, male)

-log(pValue)   2 4 6 8 10 12 14

1. Protein folding and maturation_FOMC processing
2. Immune response_Classical complement pathway
3. Immune response_Lactin induced complement pathway
4. Immune response_Alternative complement pathway
5. Immune response_ETV3 affect on CSF1-promotec macrophage differentiation
6. Immune response_MIF in innate immunity response
7. Immune response_IL-2 activation and signaling pathway
8. Reproduction_GnRH signaling
9. Immune response_IL-3 activation and signaling pathway
10. Transcription_Role of AP-1 in regulation of cellular meabolism

Pairing3 (HCV+B vs HCV+BCL, female)

-log(pValue)   2 4 6 8 10

1. immune response_NFAT in immune response
2. murine response_BCR pathway
3. murine reponse_CD28 signaling
4. murine response_T cell receptor signaling pathway
5. Cell cycle The metaphase checkpoint
6. Development_GM-CSF signaling
7. Immune response_IL-2 activation and signaling pathway
8. Cytoskelton remodeling_Cytoskelton remodeling
9. Immune response_TCR and CD28 co-stimulation in activation of NF-kB
10. Immune response_ICCS pathway in T-helper cell

Pairing 4 (HCV+ vs HCV-, B cells, female)

-log(pValue)   2 4 6 8 10

1. Cell cycle_The metaphase check point
2. Cell cycle_Chromosome condensation in prometaphase
3. Cell cycle Role of APC in cell cycle regulation
4. Cell cycle_Spindle assembly and chromosome separation
5. Cell cycle_Inhibition of mitosis
6. Immune response_Th1 and Th2 cell differentiation
7. Cell cycle_Transition and termination of DNA replication
8. Cell cycle_Cell cycle (generic shema)
9. Reproduction_Progesterone-mediated oocyte maturation
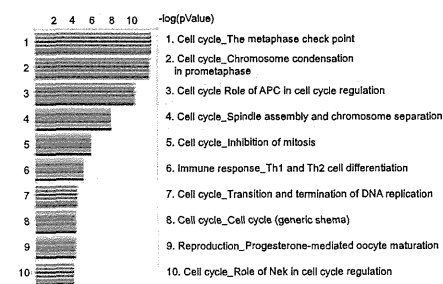10. Cell cycle_Role of Nek in cell cycle regulation

93

Figure 1. Data from array performed once with mixed RNA samples (Table 1) were analysed using MetaCore software. Signals were analysed in the disease network (**A**) and in the process network (**B**) the values for the microarray data [(Feature number; yellow), (Process Signal (635); blue), (Process signal (532); red), Test/Control (532/635); green], (Process Signal (635); orange), (Process signal (532); purple)] are indicated by coloured bars. Abbreviations: BCL = B cell lymphoma. Refer to Table 1 for construction of pairings.
doi:10.1371/journal.pone.0091373.g001

were registered in the Gene Expression Omnibus (GEO) database under the accession number GSE54722.

Quantitative RT-PCR

cDNA was synthesised from 0.5 or 1 µg of total RNA with a Superscript II kit (Life Technologies, Carlsbad, CA). TaqMan gene expression assays were custom-designed and manufactured by Life Technologies. RNA expression was quantified using the ABI 7500 real-time PCR system (Life Technologies) or the CFX96 system (BioRad, Hercules, CA).

Western blot analysis

Whole-cell proteins were extracted using RIPA buffer. Protein concentrations were determined using the BCA Protein assay Kit-Reducing Agent Compatible (Pierce Biotechnology, Rockford, IL). Samples (~10 µg) were loaded onto 10% SDS acrylamide gels, and gels were then transferred to PVDF membranes (Merck Millipore, Darmstadt, Germany). Membranes were blocked using 5% (w/v) non-fat milk for approximately 1 hour at room temperature and were then sequentially probed with primary and secondary antibodies at 4°C overnight and at room temperature for approximately 1 hour, respectively.

As primary antibodies, anti-A20 antibody (sc-166692; Santa Cruz Biotech, Dallas, TX), anti-A20 antibody (SAB3500036; Sigma-Aldrich, St. Louis, MO), anti-C3 antibody (D-19; Santa Cruz Biotech), anti-Fos (sc-52; Santa Cruz Biotech), anti-c-Jun(N) (sc-45; Santa Cruz Biotech) and anti-GAPDH-HRP (sc-20357; Santa Cruz Biotech) antibodies were used. Secondary antibodies used were horseradish peroxidase-coupled donkey anti-rabbit Ig (NA934; GE Healthcare, Buckinghamshire, UK) and horseradish peroxidase-coupled sheep anti-mouse Ig (NA931; GE Healthcare). Protein bands were detected and quantified using either Super-Signal West Dura or Femto Extended Duration Substrate (Pierce Biotechnology) with a LAS-3000 Image Analyzer (Fuji Film, Tokyo, Japan). Stripping and re-probing of the Western blots were performed using Re-blot plus mild antibody stripping solution (Merck Millipore).

Histological preparation

Liver, spleen, thymus and lymph nodes were harvested from HCV-Tg mice and fixed in 4% (wt/vol) paraformaldehyde in phosphate-buffered saline (pH 7.5) at 4°C for 24 hours. After fixation, samples were dehydrated in a graded ethanol series, cleared in xylene and embedded in paraffin, and 4-µm semi-thin sections were prepared using a carbon steel blade (Feather Safety Razor Co., Osaka, Japan) on a microtome (Yamato Kouki, Tokyo, Japan). Tissue sections were mounted on super-frosted glass slides coated with methyl-amino-silane (Matsunami Glass, Osaka, Japan). Histological images were acquired using an Olympus BX53 microscope (Olympus, Tokyo, Japan) equipped with 10×/0.30, 20×/0.50, 40×/0.75, and 100×/1.30 NA objective lenses. Images were captured using an Olympus DP73 (Olympus) under an Olympus FV1000 confocal microscope (Olympus).

Immunofluorescence

Anti-mouse NF-κB p65 antibody (Ab7970; Abcam, Cambridge, UK) and anti-mouse B220 (14-0452-81; eBioscience, San Diego, CA) were used as primary antibodies, and donkey anti-rat IgG-

Alexa Fluor 488 [712-545-153; Jackson ImmunoResearch Laboratories Inc. (JIR), West Grove, PA], donkey anti-rabbit IgG-Alexa Fluor 488 (711-545-152; JIR), donkey anti-rat IgG-Cy3 (712-165-153; JIR) and donkey anti-rabbit IgG-Cy3 (711-165-152; JIR) were used as secondary antibodies. Staining was conducted as described previously [47]. Briefly, antigen retrieval was performed in a steam pressure cooker with prewarmed antigen retrieval buffer, citrate pH 6 (S203130; Dako, Glostrup, Denmark) at 95°C for 15 min. After blocking with 3% bovine serum albumin in phosphate-buffered saline, sections (4 µm) were incubated with anti-NF-κB, -Iκ-B, -B200 or -A20 antibodies at a 1:200 dilution each at 4°C overnight. Sections were incubated with secondary antibodies and anti-rat Alexa Fluor 488, -rabbit Alexa Fluor 488, -rat Alexa Fluor 546, and -rabbit Alexa Fluor 546 at room temperature for 2 hours. Nuclei were stained with Hoechst 333421 (H3570; Life Technologies).

Single assay stem-loop Q-RT-PCR/ miR-26b analysis

Formalin-fixed, paraffin-embedded (FFPE) splenic tissue from 24 animals (BCL HCV+, n = 8; BCL HCV-, n = 5; non-tumorous spleen HCV+/−, n = 11) was selected for miR-26b expression analysis. Total RNA was extracted using an RNeasy FFPE Kit (Qiagen, Hilden, Germany) in accordance with the manufacturer's protocol. Single assay stem-loop Q-RT-PCR (TaqMan Micro-RNA assays, Life Technologies) was used to quantify miRNAs in accordance with the manufacturer's protocol. Total RNA input for each reaction was 50 ng. Expression was analysed for hsa-miR-26b and an endogenous control (snoRNA202). Each sample was analysed in triplicate, and delta C_t values were calculated using endogenous controls.
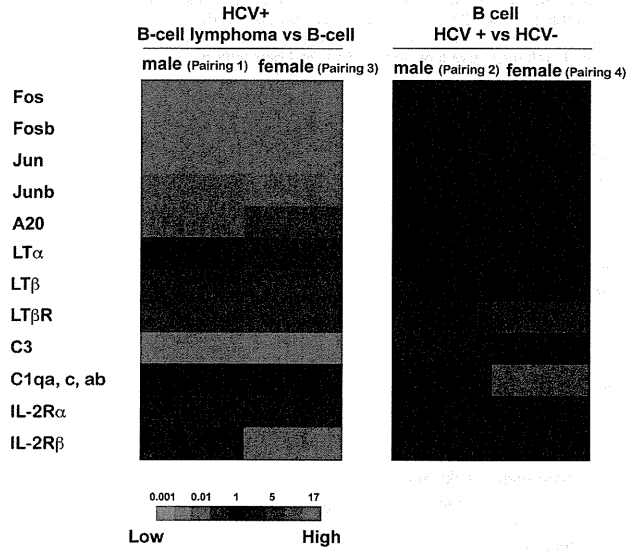
Statistics

For statistical analysis of NF-κB localisation, approximately 30–100 cells were randomly selected from each section area (two sections were used), and the cells double-positive for NF-κB and B220 were counted. All statistical analyses were performed using Prism software, version 5 (GraphPad, San Diego, CA). All experiments were independently performed three times, and a two-tailed Student t-test was applied to verify whether the results were significantly changed compared to the control (P<0.05).
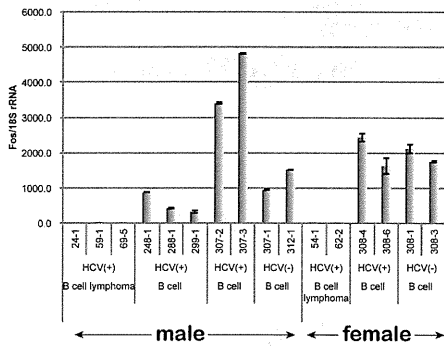
Results

Characterisation of gene expression in B cells from HCV-Tg mice by microarray analysis

We previously established HCV-Tg mice that develop spontaneous BCL with a high penetrance (approximately 25%) [43]. To clarify the mechanisms of the HCV-associated B-NHL development using this mouse model, we performed a comprehensive gene expression analysis using a genome-wide microarray. B cells were isolated from BCL-developing HCV-Tg mice (Table 1, upper columns of pairing 1 and 3), from BCL-non-developing HCV-Tg mice (lower columns of pairing 1 and 3 and upper columns of pairing 2 and 4), and from BCL-non-developing HCV-negative mice (lower columns of pairing 2 and 4). RNA was purified from these B cells (Figure S1) and was characterised by microarray analysis (data not shown). In B cells isolated from BCL-non-developing HCV-Tg male mice, 455 and 863 genes were up-
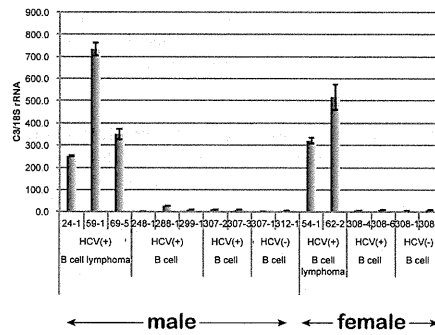
94

A
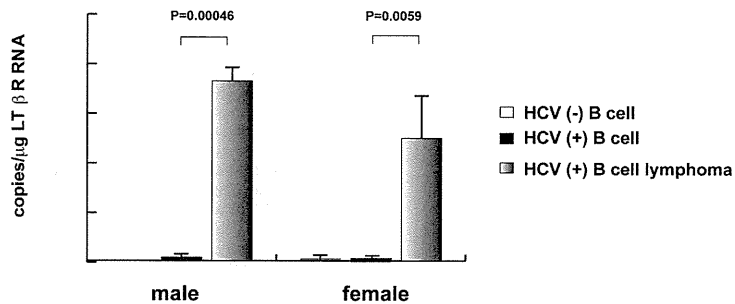

B

C

D

HCV (-) B cell
HCV (+) B cell
HCV (+) B cell lymphoma

95

and down-regulated, respectively, compared with the HCV-negative counterparts (Table 1, pairing 2); whereas 133 and 331 genes were up- and down-regulated, respectively, in BCL-non-developing HCV-Tg female mice (Table 1, pairing 4). Furthermore, 1,682 and 2,383 genes were up- and down-regulated, respectively, in BCL-developing HCV-Tg male mice compared to their BCL-non-developing counterparts (Table 1, pairing 1); whereas 2,089 and 2,565 genes were up- and down-regulated, respectively, in BCL-developing HCV-Tg female mice (Table 1, pairing 3).

Metacore analysis of microarray results

In order to characterize the cellular processes affected by the gene expression changes, we carried out a pathway analysis of microarray data of pairings 1–4 (Table 1) using MetaCore[TM] software. This data mining revealed that lymphoma, leukaemia, B cell lymphoma, and lymphatic disease pathways were appreciably modified in pairings 1 and 3 with high frequency (Figure 1a). In pairings 2 and 4, the modifications involving wound healing and infection pathways were highlighted, respectively. In the process network, the cell cycle and immune response (B cell receptor, T cell receptor, and IL-2) pathways were greatly modified in pairings 1 and 3 (Figure 1b). The immune response (complement, macrophage, IL-2, and IL-3 in group 2; Th1 and Th2 in pairing), protein folding (in pairing 2), and cell cycle (in pairing 4) pathways were also modified.

Dysregulated genes in HCV-associated B-cell lymphoma

In addition to the pathways analysis, we also carefully examined the expression of genes involved in oncogenic pathways associated with BCL. Expression of Fos, Fosb, Jun and Junb was markedly down-regulated in BCL obtained from HCV-Tg mice (Figure 2a). Similarly, the expression of A20 and LTβ was greatly down-regulated in BCL (Figure 2a). In contrast, the expression of the LTβ receptor (LTβR), the IL-2 receptor α(IL-2Rα, IL-2Rβ and complement C3 was up-regulated in the examined BCLs (Figure 2a). While alterations in the gene expression of LTα and IL-2Rβ differed between males and females, the overall mRNA expression profile in the BCL analysed from HCV-Tg mice essentially showed no differences between male and female mice. In addition, clinically, there was no clear gender priority in HCV-NHL [48–50]. These results suggest that the molecular signalling pathways leading to HCV-associated B-NHL development are common to males and females.

In non-tumorous B cells from BCL-non-developing HCV-Tg male mice, the expression of LTβR and C3 was up-regulated when compared with HCV-negative counterparts (Figure 2a). In contrast, in female counterparts, the expression of LTβR and complements C1qa, c, and ab was down-regulated (Figure 2a, Pair. 4). These results suggest that the impact of HCV infection in B cells may be different between males and females.

Expression of Fos, C3, and LTβR genes in HCV-associated BCL

In order to validate the microarray results, levels of Fos and C3 mRNAs were quantified by real-time PCR. Striking down-regulation of Fos gene expression was observed in BCLs from HCV-Tg mice (Figure 2b). In contrast, C3 mRNA expression was markedly up-regulated in BCLs from HCV-Tg mice (Figure 2c). These results were consistent with the microarray data (Figure 2a, GEO accession number GSE54722). Similarly, the mRNA expression of the LTβR gene was significantly increased in HCV-associated BCLs (Figure 2d), confirming the microarray analysis results (Figure 2a). Importantly, these changes occurred in both male and female mice.
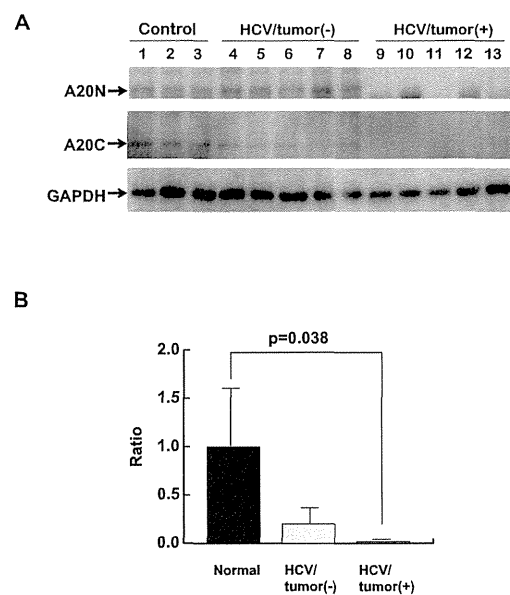
Figure 3. The expression of A20 in HCV-associated BCL. A: Expression levels of A20 in the spleen from RzCD19Cre mice with or without BCL. Whole-tissue extracts prepared from the spleen in CD19Cre mice (control, n=3; lanes 1–3 217-2, 2 224-2, 224-3), RzCD19Cre mice without BCL (HCV/Tumour(-), n=5; lanes 4–8 217-3, 224-4, 232-3, 254-4, 240-2) and RzCD19Cre mice with BCL (HCV/Tumour(+), n=5; lanes 9–13 24-1, 56-5, 69-5, 59-1, 43-4) were subjected to SDS-PAGE and were analysed by immunoblotting using anti-N terminal (A20N), anti-C terminal A20 (A20C), and anti-GAPDH antibodies. GAPDH was used as protein loading control. **B:** Quantitation of A20 (N and C), the average is indicated and statistical analysis was performed. Vertical bars indicate S.D.
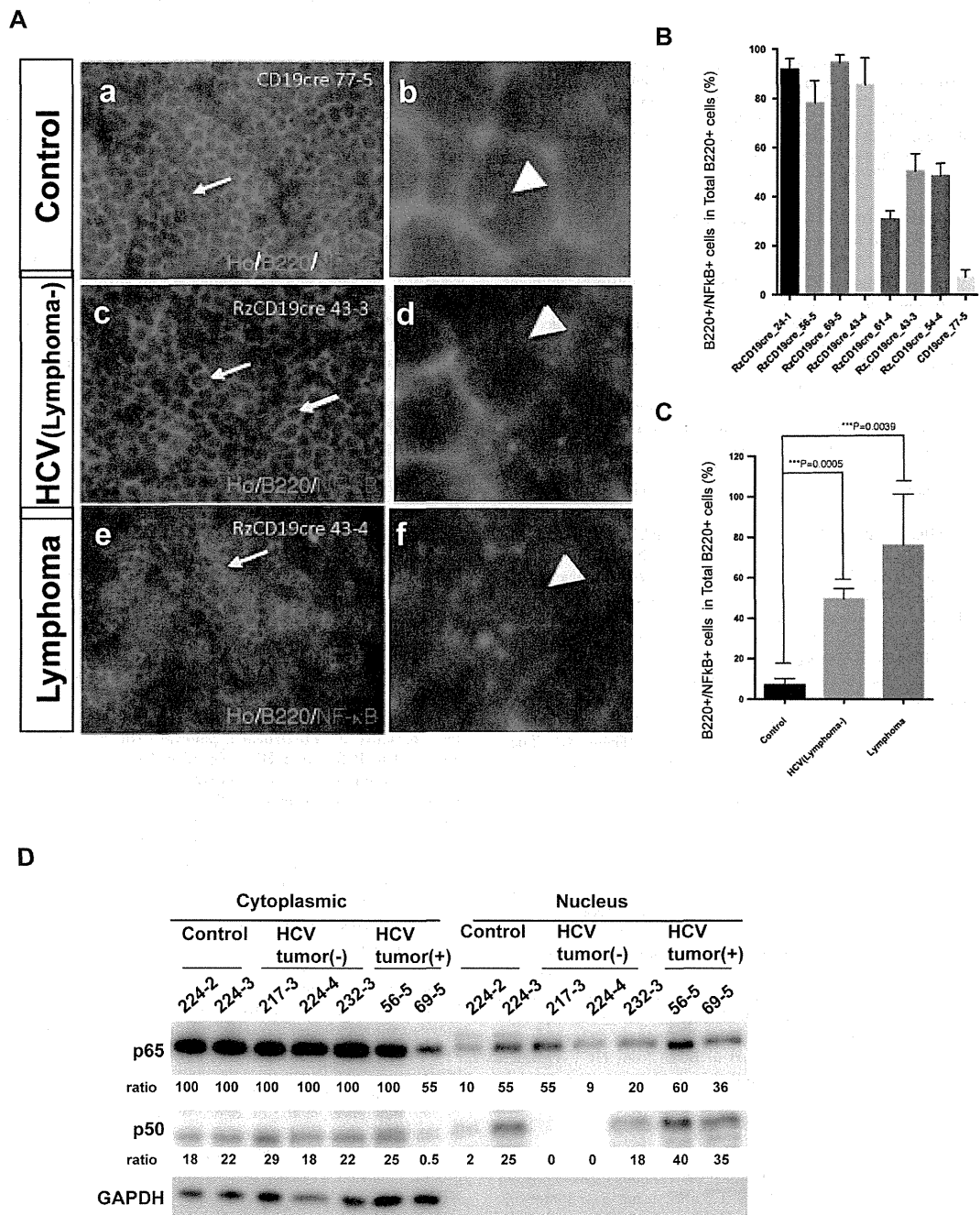doi:10.1371/journal.pone.0091373.g003

96

Figure 4. Double immunofluorescence localisation of B220 (Green) and NF-κB p65 (Red) in HCV-Tg mice and the fractionation analysis of mouse tissues. A: Co-localisation of NF-κB p65 immunoreactivity with B220 is indicated by arrows. (a–b) Cells double-positive for B220 and NF-κB in the control mouse (CD19cre). (c–d) Cells double-positive for B220 and NF-κB in the asymptomatic HCV-Tg mouse (RzCD19cre). (e–f) Cells double-positive for B220 and NF-κB in the lymphomatous HCV-Tg mouse (RzCD19cre). **B:** Quantitative analysis of the ratio of double-positive

97

cells among B220-positive cells in each HCV-Tg mouse. Bar graph indicates the percentage of cells with NF-κB p65 nuclear translocation in B220-positive cells. C: Bar graph shows the ratio of double-positive cells within the B220-positive cells in normal, asymptomatic and lymphomatous HCV-Tg mice. Ho: Hoechst33342 Data are presented as means ± S.E., * P<0.05, ** P<0.01, *** P<0.001. D: Western blot analysis: tissues from the spleen of controls (224-2, 3) or HCV-Tg mice without BCL (217-3, 224-4, 232-3) or with BCL (56-5, 69-5) were fractionated into nuclear and cytoplasmic fractions. NF-κB p50 and p65 were detected by antibodies. Relative ratios of quantitation by imager are indicated. GAPDH was detected as a loading control of the cytoplasmic fraction.
doi:10.1371/journal.pone.0091373.g004

Expression of A20 in HCV-associated BCL

In order to further validate the microarray results, we assessed A20 protein levels in BCLs isolated from HCV-Tg mice by Western blotting (Figure 3a). Two distinct anti-A20 antibodies recognising the N- (A20N) and C-terminal regions were used for the detection of A20. Regardless of the anti-A20 antibodies used, expression levels of A20 in BCL from HCV-Tg mice (Figure 3a, lanes 9 to 13) were markedly decreased when compared to splenocytes obtained from either BCL-non-developing HCV-negative mice (lanes 1 to 3) or from BCL-non-developing HCV-Tg mice (lanes 4 to 8). Quantitative analysis showed a significant decrease in A20 in BCLs obtained from HCV-Tg mice (Figure 3b). These results strongly suggest that the reduced expression of A20 is correlated with HCV-associated N-BHL development.

Nuclear localisation of NF-kB p65 in HCV-associated BCL

We next analysed the activation status of NF-κB by investigating the nuclear localisation of NF-κB p65 in cells positive for a B-cell marker molecule, B220, in BCLs isolated from HCV-Tg mice (Figure 4a). Quantitative analysis revealed that the ratio of cells double-positive for B220 and NF-κB p65 in the nuclei of the examined BCLs was significantly higher than the ratio in splenic tissue obtained from either BCL-non-developing HCV-negative mice or from BCL-non-developing HCV-Tg mice (Figures 4b and c). The fractionation assay showed that more NF-κB p50 and p65 were present in BCLs from HCV-Tg mice (Figure 4d). These results indicate the activation of NF-κB in HCV-associated BCL.

Expression of miR-26b in HCV-associated BCL

Recent studies have demonstrated that miR-26b is down-regulated in hepatocellular carcinoma [51], nasopharyngeal carcinoma [52], primary squamous cell lung carcinoma [53] and squamous cell carcinoma of the tongue [54]. In addition, miR-26b was down-regulated in HCV-positive SMZL when compared with HCV-negative counterparts [41] and in the PBMC of HCV-positive MC and NHL patients [42]. Therefore, we compared the expression levels of miR-26b in BCL from HCV-Tg mice with BCL from HCV-negative mice (i.e., spontaneously developed BCL) or in splenic tissue from BCL non-developing HCV-positive and -negative mice (Figure. 5). Interestingly, miR-26b expression was significantly down-regulated in BCLs from HCV-Tg mice. These results indicate that miR-26b is also down-regulated in HCV-associated BCL.

Discussion

In the present study, we identified differentially expressed genes in BCLs examined from HCV-Tg mice using a genome-wide microarray (Figures 1 and 2a, Table 1, and Figure S2). The microarray results for representative genes were validated at the RNA (Figures 2 and 5) and protein (Figures 3 and 4) levels. These findings helped dissect the molecular mechanisms underlying HCV-associated B-NHL development.

In the BCLs from HCV-Tg mice, the marked down-regulation of the Fos gene as well as other AP-1 protein genes (Fosb, Jun and Junb) was observed. Although AP-1 DNA binding activity was

observed in Hodgkin-/multinuclear Reed-Stemberg cells and tissues from classical Hodgkin's disease, non-Hodgkin cell lines lacked the DNA binding activity of AP-1 [55]. Junb was weakly expressed in non-Hodgkin lymphomas of B-lymphoid origin; however, strong expression has been previously found in lymphomas that originated from the T-lymphoid lineage, and Junb selectively blocked B-lymphoid but not T-lymphoid cell proliferation ex vivo [56]. The BCL that developed in HCV-Tg mice was the non-Hodgkin type [43]; therefore, the decrease in AP-1 protein levels (Fos, Fosb, Jun, and Junb) may be crucial for lymphoma development.

In our previous study, soluble IL-2Rα levels were increased in BCL-developing HCV-Tg mice [43] Therefore, the up-regulation of IL-2Rα(Figure 2a) is potentially linked to the increase of soluble IL-2Rα, although further investigation is needed to clarify the details of this mechanism.

Expression of complement component C3 was significantly increased in BCLs isolated from HCV-Tg mice (Figure 2c). The presence of polymorphisms in complement system genes in non-Hodgkin lymphoma [57] suggests the involvement of complement in lymphoma development. The elevated C3 expression may be induced by TNF-α [58]. In addition, C3a, which is a cleavage product of C3, may contribute to the binding of NF-κB and AP-1 as shown previously [59].

The expression of LTβR, which is one of the key molecules in the alternative NF-κB signalling pathway [16], was significantly increased in BCLs from HCV-Tg mice (Figure 2d). HCV core proteins were reported to interact with the cytoplasmic domain of LTβR [60,61] and to enhance the alternative NF-κB signalling pathway [62]. The induction of LTβR by the HCV non-structural protein NS5B, and HCV RNA-dependent RNA polymerase, was also observed [63]. These findings suggest that the regulatory pathways involved in HCV infection also play a role in HCV-associated B-NHL development.

We observed several differences in the gene expression between male and female mice. Male HCV-negative mice showed up-regulation of LTβR and C3; however, female HCV-positive mice featured the downregulation of LTα and up-regulation of IL-2Rβ. Female HCV-Tg mice showed decreased overall survival in a previous study [43] and the above-mentioned gene dysregulations may contribute to this finding. However, the incidence of B-NHL between male and female mice did not show marked differences in the transgenic model [43]. Some clinical studies found gender-specific differences in the incidence of HCV-associated B-NHL and different effects of HCV on gene expression, which may also be dependent on gender [64]. However, meta-analyses did not provide consistent evidence for any gender preferences in HCV-NHL [48–50].

The down-regulation of A20, which is a ubiquitin-editing enzyme and tumour suppressor in various lymphomas [26], was observed in BCLs from HCV-Tg mice (Figures 3a and 3b). A20 has been reported to interact with the TNF receptor associated factor 2 (TRAF2), TRAF6, and the NF-κB essential modulator (NEMO). A20 inhibits NF-κB activation-induced by TNFα or by the overexpression of other proteins such as TRAF2 and receptor-interacting protein serine/threonine kinase 1 (RIPK1) proteins
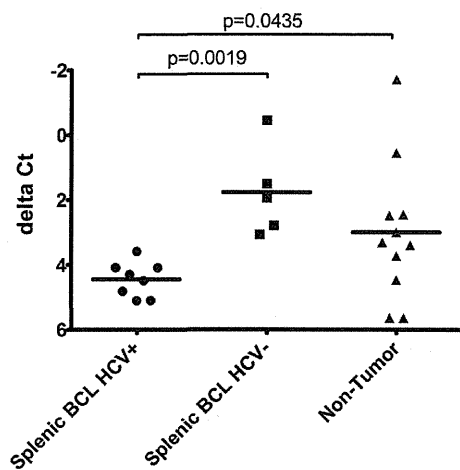
98

Figure 5. Quantification of miR-26b in BCL from HCV-positive and HCV-negative and non-tumour Tg mice. Formalin-fixed, paraffin-embedded (FFPE) splenic tissue from 24 animals (BCL HCV+, n = 8; BCL HCV-, n = 5; non-tumorous spleen HCV+/−, n = 11) was analysed for miR-26b expression by single assay stem-loop Q-RT-PCT by triplicate experiments. Data are shown as scatter dot-plots, and horizontal bar depicts the mean; y-axis: delta Ct (inverted scale) calculated in relation to endogenous control (snoRNA202). HCV-positive lymphoma tissue: filled circles; HCV-negative lymphoma tissue: filled squares; non-tumorous splenic tissue: filled triangles. P-values are shown in the graph.
doi:10.1371/journal.pone.0091373.g005

[65]. RIPK3 contributes to TNFR1-mediated RIPK1-dependent apoptosis and necroptosis [66]. RIPK2 (also known as RIP2) is also involved in B cell lymphoma cell survival and mediates the activation of NF-κB and MAPK pathways, associated with the TNF receptor family [67]. Therefore, suppression of A20 activates NF-κB by increasing nuclear translocation in tumour tissues.

Expression of miR-26b in BCLs obtained from HCV-Tg mice was significantly down-regulated (Figure 5). miR-26b is also down-regulated in numerous cancers, e.g., HCC [51], nasopharyngeal carcinomas [52], primary squamous cell lung carcinomas [53]and squamous cell carcinoma tongue [54]. In addition, c-Myc, which is up-regulated in various cancer types, has been shown to contribute to the reduction of miR-26a/b expression [68]. Notably, expression of miR-26b was significantly down-regulated in SMZL arising in HCV-positive patients [41]. Although the mechanisms

of miR-26b-mediated tumourigenicity regulation are not fully understood, previous reports [69] and the present study have suggested a possible regulatory role of miR-26b in HCV-related lymphoma. Several candidates are reported to be targets of miR-26b. miR-26a and miR-26b are regulators of EZH2, which is the PRC2 polycomb repressive complex, is overexpressed in multiple cancers and is a target of the MYC oncogene [70]. In addition, lymphoid enhancer factor (LEF)-1 [42] and Nek6 [41] are targets of miR-26b. LEF-1 is a nuclear transcription factor that forms a complex with β-catenine and T-cell factor and induces transcription of cyclin D1 and c-myc. Nek6 is a kinase involved in the initiation of mitosis and is overexpressed in various tumours. The phosphatase and tensin homolog gene (PTEN) is also the putative target gene of miR-26b in adipogenic regulation [71] and cell growth [72].

This report is the first to demonstrate the possible involvement of networks of NF-κB, AP-1, complements and miR-26b in HCV-associated B-NHL (Figure S2). A future study focusing on the dysregulation of these networks and their modification by HCV may provide valuable information on improving therapy for HCV-associated B-NHL.

Supporting Information

Figure S1 A: B cells were isolated from mice using MACS beads and anti-CD19 antibody. The population of B cells was confirmed by staining with anti-B220 antibody. **B:** RNA integrity number (RIN) was measured using an Agilent 2100 Bioanalyzer (Agilent) for the estimation of purity.
(PDF)

Figure S2 Possible pathways involved in BCL development. Both canonical and alternative NF-κB pathways may play a role. Bold arrows indicate up-regulation or down-regulation. NIK; NF-κB-inducing kinase.
(PDF)

Acknowledgments

Author Contributions

Conceived and designed the experiments: KT-K T. Mizuochi. Performed the experiments: YK T. Mizukami HK JP-O KT-K. Analyzed the data: YN JP-O T. Mizuochi KT-K. Contributed reagents/materials/analysis tools: MK. Wrote the paper: MO JP-O T. Mizuochi KT-K.

References

1. Shepard CW, Finelli L, Alter MJ (2005) Global epidemiology of hepatitis C virus infection. Lancet Infect Dis 5: 558–567.
2. Libra M, Gasparotto D, Gloghini A, Navolanic PM, De Re V, et al. (2005) Hepatitis C virus (HCV) I hepatitis C virus (HCV) infection and lymphoproliferative disorders. Front Biosci 10: 2460–2471.
3. Saito I, Miyamura T, Ohbayashi A, Harada H, Katayama T, et al. (1990) Hepatitis C virus infection is associated with the development of hepatocellular carcinoma. Proc Natl Acad Sci U S A 87: 6547–6549.
4. Silvestri F, Pipan C, Barillari G, Zaja F, Fanin R, et al. (1996) Prevalence of hepatitis C virus infection in patients with lymphoproliferative disorders. Blood 87: 4296–4301.
5. Ascoli V, Lo Coco F, Artini M, Levrero M, Martelli M, et al. (1998) Extranodal lymphomas associated with hepatitis C virus infection. Am J Clin Pathol 109: 600–609.
6. Mele A, Pulsoni A, Bianco E, Musto P, Szklo A, et al. (2003) Hepatitis C virus and B-cell non-Hodgkin lymphomas: an Italian multicenter case-control study. Blood 102: 996–999.

7. Ito M, Kusunoki H, Mizuochi T (2011) Peripheral B cells as reservoirs for persistent HCV infection. Front Microbiol 2: 177.
8. Dammacco F, Sansonno D, Piccoli C, Racanelli V, D'Amore FP, et al. (2000) The lymphoid system in hepatitis C virus infection: autoimmunity, mixed cryoglobulinemia, and Overt B-cell malignancy. Semin Liver Dis 20: 143–157.
9. Peveling-Oberhag J, Arcaini L, Hansmann ML, Zeuzem S (2013) Hepatitis C-associated B-cell non-Hodgkin lymphomas. Epidemiology, molecular signature and clinical management. J Hepatol 59: 169–177.
10. Hermine O, Lefrere F, Bronowicki JP, Mariette X, Jondeau K, et al. (2002) Regression of splenic lymphoma with villous lymphocytes after treatment of hepatitis C virus infection. N Engl J Med 347: 89–94.
11. Hess J, Angel P, Schorpp-Kistner M (2004) AP-1 subunits: quarrel and harmony among siblings. J Cell Sci 117: 5965–5973.
12. Vasanwala FH, Kusam S, Toney LM, Dent AL (2002) Repression of AP-1 function: a mechanism for the regulation of Blimp-1 expression and B lymphocyte differentiation by the B cell lymphoma-6 protooncogene. J Immunol 169: 1922–1929.

99

13. Pekarsky Y, Palamarchuk A, Maximov V, Efanov A, Nazaryan N, et al. (2008) Tcl1 functions as a transcriptional regulator and is directly involved in the pathogenesis of CLL. Proc Natl Acad Sci U S A 105: 19643–19648.

14. Ghosh S, Karin M (2002) Missing pieces in the NF-kappaB puzzle. Cell 109 Suppl: S81–96.

15. Sen R, Baltimore D (1986) Inducibility of kappa immunoglobulin enhancer-binding protein NF-kappa B by a posttranslational mechanism. Cell 47: 921–928.

16. Bakkar N, Guttridge DC (2010) NF-kappaB signaling: a tale of two pathways in skeletal myogenesis. Physiol Rev 90: 495–511.

17. Sun B, Karin M (2008) NF-kappaB signaling, liver disease and hepatoprotective agents. Oncogene 27: 6228–6244.

18. Arsura M, Cavin LG (2005) Nuclear factor-kappaB and liver carcinogenesis. Cancer Lett 229: 157–169.

19. Haybaeck J, Zeller N, Wolf MJ, Weber A, Wagner U, et al. (2009) A lymphotoxin-driven pathway to hepatocellular carcinoma. Cancer Cell 16: 295–308.

20. De Re V, Caggiari L, Garziera M, De Zorzi M, Repetto O (2012) Molecular signature in HCV-positive lymphomas. Clin Dev Immunol 2012: 623465.

21. Opipari AW, Jr., Boguski MS, Dixit VM (1990) The A20 cDNA induced by tumor necrosis factor alpha encodes a novel type of zinc finger protein. J Biol Chem 265: 14705–14708.

22. Song HY, Rothe M, Goeddel DV (1996) The tumor necrosis factor-inducible zinc finger protein A20 interacts with TRAF1/TRAF2 and inhibits NF-kappaB activation. Proc Natl Acad Sci U S A 93: 6721–6725.

23. Lee EG, Boone DL, Chai S, Libby SL, Chien M, et al. (2000) Failure to regulate TNF-induced NF-kappaB and cell death responses in A20-deficient mice. Science 289: 2350–2354.

24. Heyninck K, Beyaert R (2005) A20 inhibits NF-kappaB activation by dual ubiquitin-editing functions. Trends Biochem Sci 30: 1–4.

25. Malynn BA, Ma A (2009) A20 takes on tumors: tumor suppression by an ubiquitin-editing enzyme. J Exp Med 206: 977–980.

26. Hymowitz SG, Wertz IE (2010) A20: from ubiquitin editing to tumour suppression. Nat Rev Cancer 10: 332–341.

27. Kato M, Sanada M, Kato I, Sato Y, Takita J, et al. (2009) Frequent inactivation of A20 in B-cell lymphomas. Nature 459: 712–716.

28. Honma K, Tsuzuki S, Nakagawa M, Karnan S, Aizawa Y, et al. (2008) TNFAIP3 is the target gene of chromosome band 6q23.3-q24.1 loss in ocular adnexal marginal zone B cell lymphoma. Genes Chromosomes Cancer 47: 1–7.

29. Honma K, Tsuzuki S, Nakagawa M, Tagawa H, Nakamura S, et al. (2009) TNFAIP3/A20 functions as a novel tumor suppressor gene in several subtypes of non-Hodgkin lymphomas. Blood 114: 2467–2475.

30. Schmitz R, Hansmann ML, Bohle V, Martin-Subero JI, Hartmann S, et al. (2009) TNFAIP3 (A20) is a tumor suppressor gene in Hodgkin lymphoma and primary mediastinal B cell lymphoma. J Exp Med 206: 981–989.

31. Compagno M, Lim WK, Grunn A, Nandula SV, Brahmachary M, et al. (2009) Mutations of multiple genes cause deregulation of NF-kappaB in diffuse large B-cell lymphoma. Nature 459: 717–721.

32. Parvatiyar K, Barber GN, Harhaj EW (2010) TAX1BP1 and A20 inhibit antiviral signaling by targeting TBK1-IKKi kinases. J Biol Chem 285: 14999–15009.

33. Parvatiyar K, Harhaj EW (2011) Regulation of inflammatory and antiviral signaling by A20. Microbes Infect 13: 209–215.

34. Tavares RM, Turer EE, Liu CL, Advincula R, Scapini P, et al. (2010) The ubiquitin modifying enzyme A20 restricts B cell survival and prevents autoimmunity. Immunity 33: 181–191.

35. Verstrepen L, Verhelst K, van Loo G, Carpentier I, Ley SC, et al. (2010) Expression, biological activities and mechanisms of action of A20 (TNFAIP3). Biochem Pharmacol 80: 2009–2020.

36. He L, Hannon GJ (2004) MicroRNAs: small RNAs with a big role in gene regulation. Nat Rev Genet 5: 522–531.

37. Lawrie CH (2007) MicroRNA expression in lymphoma. Expert Opin Biol Ther 7: 1363–1374.

38. Jopling CL, Yi M, Lancaster AM, Lemon SM, Sarnow P (2005) Modulation of hepatitis C virus RNA abundance by a liver-specific MicroRNA. Science 309: 1577–1581.

39. Kim SW, Ramasamy K, Bouamar H, Lin AP, Jiang D, et al. (2012) MicroRNAs miR-125a and miR-125b constitutively activate the NF-kappaB pathway by targeting the tumor necrosis factor alpha-induced protein 3 (TNFAIP3, A20). Proc Natl Acad Sci U S A 109: 7865–7870.

40. Hother C, Rasmussen PK, Joshi T, Reker D, Ralfkiaer U, et al. (2013) MicroRNA Profiling in Ocular Adnexal Lymphoma: A Role for MYC and NFKB1 Mediated Dysregulation of MicroRNA Expression in Aggressive Disease. Invest Ophthalmol Vis Sci 54: 5169–5175.

41. Peveling-Oberhag J, Crisman G, Schmidt A, Doring C, Lucioni M, et al. (2012) Dysregulation of global microRNA expression in splenic marginal zone lymphoma and influence of chronic hepatitis C virus infection. Leukemia 26: 1654–1662.

42. Fognani E, Giannini C, Piluso A, Gragnani L, Monti M, et al. (2013) Role of microRNA profile modifications in hepatitis C virus-related mixed cryoglobulinemia. PLoS One 8: e62965.

43. Kasama Y, Sekiguchi S, Saito M, Tanaka K, Satoh M, et al. (2010) Persistent expression of the full genome of hepatitis C virus in B cells induces spontaneous development of B-cell lymphomas in vivo. Blood 116: 4926–4933.

44. Tsukiyama-Kohara K, Tone S, Maruyama I, Inoue K, Katsume A, et al. (2004) Activation of the CKI-CDK-Rb-E2F pathway in full genome hepatitis C virus-expressing cells. J Biol Chem 279: 14531–14541.

45. Rickert RC, Roes J, Rajewsky K (1997) B lymphocyte-specific, Cre-mediated mutagenesis in mice. Nucleic Acids Res 25: 1317–1318.

46. Nishimura T, Kohara M, Izumi K, Kasama Y, Hirata Y, et al. (2009) Hepatitis C virus impairs p53 via persistent overexpression of 3beta-hydroxysterol Delta24-reductase. J Biol Chem 284: 36442–36452.

47. Yamazaki J, Mizukami T, Takizawa K, Kuramitsu M, Momose H, et al. (2009) Identification of cancer stem cells in a Tax-transgenic (Tax-Tg) mouse model of adult T-cell leukemia/lymphoma. Blood 114: 2709–2720.

48. Gisbert JP, Garcia-Buey L, Pajares JM, Moreno-Otero R (2003) Prevalence of hepatitis C virus infection in B-cell non-Hodgkin's lymphoma: systematic review and meta-analysis. Gastroenterology 125: 1723–1732.

49. Matsuo K, Kusano A, Sugumar A, Nakamura S, Tajima K, et al. (2004) Effect of hepatitis C virus infection on the risk of non-Hodgkin's lymphoma: a meta-analysis of epidemiological studies. Cancer Sci 95: 745–752.

50. de Sanjose S, Benavente Y, Vajdic CM, Engels EA, Morton LM, et al. (2008) Hepatitis C and non-Hodgkin lymphoma among 4784 cases and 6269 controls from the International Lymphoma Epidemiology Consortium. Clin Gastroenterol Hepatol 6: 451–458.

51. Ji J, Shi J, Budhu A, Yu Z, Forgues M, et al. (2009) MicroRNA expression, survival, and response to interferon in liver cancer. N Engl J Med 361: 1437–1447.

52. Ji Y, He Y, Liu L, Zhong X (2010) MiRNA-26b regulates the expression of cyclooxygenase-2 in desferrioxamine-treated CNE cells. FEBS Lett 584: 961–967.

53. Gao W, Shen H, Liu L, Xu J, Xu J, et al. (2011) MiR-21 overexpression in human primary squamous cell lung carcinoma is associated with poor patient prognosis. J Cancer Res Clin Oncol 137: 557–566.

54. Wong TS, Liu XB, Wong BY, Ng RW, Yuen AP, et al. (2008) Mature miR-184 as Potential Oncogenic microRNA of Squamous Cell Carcinoma of Tongue. Clin Cancer Res 14: 2588–2592.

55. Mathas S, Hinz M, Anagnostopoulos I, Krappmann D, Lietz A, et al. (2002) Aberrantly expressed c-Jun and JunB are a hallmark of Hodgkin lymphoma cells, stimulate proliferation and synergize with NF-kappa B. EMBO J 21: 4104–4113.

56. Szremska AP, Kenner L, Weisz E, Ott RG, Passegue E, et al. (2003) JunB inhibits proliferation and transformation in B-lymphoid cells. Blood 102: 4159–4165.

57. Bassig BA, Zheng T, Zhang Y, Berndt SI, Holford TR, et al. (2012) Polymorphisms in complement system genes and risk of non-Hodgkin lymphoma. Environ Mol Mutagen 53: 145–151.

58. Andoh A, Fujiyama Y, Hata K, Araki Y, Takaya H, et al. (1999) Counter-regulatory effect of sodium butyrate on tumour necrosis factor-alpha (TNF-alpha)-induced complement C3 and factor B biosynthesis in human intestinal epithelial cells. Clin Exp Immunol 118: 23–29.

59. Fischer WH, Jagels MA, Hugli TE (1999) Regulation of IL-6 synthesis in human peripheral blood mononuclear cells by C3a and C3a(desArg). J Immunol 162: 453–459.

60. Matsumoto M, Hsieh TY, Zhu N, VanArsdale T, Hwang SB, et al. (1997) Hepatitis C virus core protein interacts with the cytoplasmic tail of lymphotoxin-beta receptor. J Virol 71: 1301–1309.

61. Chen CM, You LR, Hwang LH, Lee YH (1997) Direct interaction of hepatitis C virus core protein with the cellular lymphotoxin-beta receptor modulates the signal pathway of the lymphotoxin-beta receptor. J Virol 71: 9417–9426.

62. You LR, Chen CM, Lee YH (1999) Hepatitis C virus core protein enhances NF-kappaB signal pathway triggering by lymphotoxin-beta receptor ligand and tumor necrosis factor alpha. J Virol 73: 1672–1681.

63. Simonin Y, Vegna S, Akkari L, Gregoire D, Antoine E, et al. (2013) Lymphotoxin Signaling Is Initiated by the Viral Polymerase in HCV-linked Tumorigenesis. PLoS Pathog 9: e1003234.

64. Vladareanu AM, Ciufu C, Neagu AM, Onisai M, Bumbea H, et al. (2010) The impact of hepatitis viruses on chronic lymphoproliferative disorders—preliminary results. J Med Life 3: 320–329.

65. Heyninck K, De Valck D, Vanden Berghe W, Van Criekinge W, Contreras R, et al. (1999) The zinc finger protein A20 inhibits TNF-induced NF-kappaB-dependent gene expression by interfering with an RIP- or TRAF2-mediated transactivation signal and directly binds to a novel NF-kappaB-inhibiting protein ABIN. J Cell Biol 145: 1471–1482.

66. Dondelinger Y, Aguileta MA, Goossens V, Dubuisson C, Grootjans S, et al. (2013) RIPK3 contributes to TNFR1-mediated RIPK1 kinase-dependent apoptosis in conditions of cIAP1/2 depletion or TAK1 kinase inhibition. Cell Death Differ 20: 1381–1392.

67. Cai X, Du J, Liu Y, Xia W, Liu J, et al. (2013) Identification and characterization of receptor-interacting protein 2 as a TNFR-associated factor 3 binding partner. Gene 517: 205–211.

68. Zhu Y, Lu Y, Zhang Q, Liu JJ, Li TJ, et al. (2012) MicroRNA-26a/b and their host genes cooperate to inhibit the G1/S transition by activating the pRb protein. Nucleic Acids Res 40: 4615–4625.

69. Ma YL, Zhang P, Wang F, Moyer MP, Yang JJ, et al. (2011) Human embryonic stem cells and metastatic colorectal cancer cells shared the common endogenous human microRNA-26b. J Cell Mol Med 15: 1941–1954.

100

70. Koh CM, Iwata T, Zheng Q, Bethel C, Yegnasubramanian S, et al. (2011) Myc enforces overexpression of EZH2 in early prostatic neoplasia via transcriptional and post-transcriptional mechanisms. Oncotarget 2: 669–683.

71. Song G, Xu G, Ji C, Shi C, Shen Y, et al. (2014) The role of microRNA-26b in human adipocyte differentiation and proliferation. Gene 533: 481–487.

72. Palumbo T, Faucz FR, Azevedo M, Xekouki P, Iliopoulos D, et al. (2013) Functional screen analysis reveals miR-26b and miR-128 as central regulators of

pituitary somatomammotrophic tumor growth through activation of the PTEN-AKT pathway. Oncogene 32: 1651–1659.

73. Tsukiyama-Kohara K, Poulin F, Kohara M, DeMaria CT, Cheng A, et al. (2001) Adipose tissue reduction in mice lacking the translational inhibitor 4E-BP1. Nat Med 7: 1128–1132.

101